



# Auroral alert version 1.0: Two-step automatic detection of sudden auroral intensification from all-sky jpeg images

Masatoshi Yamauchi and Urban Brändström

Swedish Institute of Space Physics, Bengt Hultqvist vägen 1, Box 812, S-98128 Kiruna, Sweden

**Correspondence:** M. Yamauchi (M.Yamauchi@irf.se)

**Abstract.** A real-time alert system of sudden and significant intensification of auroral arc with expanding motion (we call it "Local-Arc-Breaking" hereafter) was developed for Kiruna all-sky camera (ASC) using ASC jpeg images. The identification is made in two steps: (1) Using an "expert system" in which a combinations of simple criteria is applied to each pixels with calculations afterward (expert system), each jpeg image of the ASC is converted into a simple set of numbers, or "ASC auroral index", representing the occupancy of auroral pixels and characteristic intensity of the brightest aurora in the image. (2) Using this ASC auroral index, the level of auroral activity is estimated, aiming Level 6 as clear Local-Arc-Breaking and Level 4 as precursor for it (reserving Levels 1-3 for less active aurorae).

The first step is further divided into two stages: (1a) Using simple criteria for R (red), G (green), B (blue), and H (hue) values in the RGB and HLS colour codes, each pixel of a jpeg image is classified into several categories according to its colour as "visible diffuse", "green arc", "strong aurora" (which means saturated or mixed with  $N_2$  red line at 670 nm), "cloud", "artificial light", and "moon". (1b) The percentage of the occupying area (pixel coverage) for each category and the characteristic intensity of "strong aurora" are calculated.

The obtained ASC aurora index is posted in both a ascii format and plots on a real-time bases at <https://www.irf.se/alis/allsky/nowcast/>. When Level 6 is detected, automatic alert E-mail is sent out to the registered addresses immediately. The alert system started 5 November, 2021, and the results (both Level 6 detection and Level 4 detection) were compared to the manual (eye-)identification of the auroral activity during the rest of the auroral season of Kiruna ASC (i.e., total five months until April 2022). Unless the Moon or cloud blocks the brightened region, nearly one-to-one correspondence between Level 6 and Local-Arc-Breaking judged by original ASC images is achieved within ten minutes uncertainty.

## 1 Introduction

In spaceweather monitoring and real-time studies of the ionospheric/magnetospheric science, nowcast the local geomagnetic and ionospheric conditions is as important as monitoring the upstream conditions such as the solar wind conditions including the interplanetary magnetic field (IMF) at the Sun-Earth Lagrange (L1) point or even the detection of the coronal mass ejection (CME) and the solar flare at the Sun. While the upstream monitor provides predictions of global activities, local activities are difficult to predict even if it is a part of the predicted global activity such as a substorm, with uncertainty of more than at least 30 min and few degree in latitude and longitude. This mean that the location and timing are difficult to predict by more than this



uncertainty even for events with high risk of the space weather hazards. For such local forecast, nowcast of the local condition (such as the geomagnetic field and all-sky cameras (ASC) images) and comparing it with upstream conditions and regional conditions (area covered by several stations) are essential.

This is why many high-latitude observatories started nowcasting the local auroral conditions as soon as the internet technology becomes ready. Even data from regional network of observations such as geomagnetic array (Friis-Christensen et al., 1988; Luhr et al., 1998) and ASC array (Syrjäsuo et al., 1998; Partamies et al., 2003) are being nowcasted, updating every minute or even more frequent. In addition, some observatory nowcast the keograms of these ASCs over north-south directions. These data are also archived and being used for auroral, ionospheric, and magnetospheric researches, including event searching.

The handiness of ASC data also stimulated non-specialist of aurora to use ASC data. These potential users includes electric power companies, satellite community (scientists, engineers, and operators) except those engaged with optical instruments, and even tourists and aurora enthusiast. However, these potential users are normally not familiar to interpreting the ASC auroral images nor keograms. Considering wide possible users, the activity level of the aurora in addition to the keograms should also be nowcasted as a simple manner as possible.

One way is producing an index that is composed of a simple set of numbers. The idea is similar to real-time AE nowcast by the world data center (WDC) in Kyoto ([http://wdc.kugi.kyoto-u.ac.jp/ae\\_realtime/presentmonth/index.html](http://wdc.kugi.kyoto-u.ac.jp/ae_realtime/presentmonth/index.html)) for auroral region and real-time Kp nowcast by Helmholtz Centre in Potsdam (<https://isdg.gfz-potsdam.de/kp-index/>) sub-auroral region. Another analogy is the moment data (density, velocity, pressure) calculated from particle spectrometer. Such an "index" allows even auroral scientists to overview the activity during the recent one hour through line plots of the index values.

In both the geomagnetic indices and moment values, these simplified "numbers" are used to judge the level of geomagnetic and plasma activities, respectively. Likewise, the set of numbers calculated from the ASC images can be used to evaluate the auroral activity level, such as the sudden and significant intensification of auroral arc with expanding motion (we call it "Local-Arc-Breaking" hereafter). This "second step" classification opens up a possibility of the real-time alert of large activities. The concept of this classification in terms of level is similar to the "class" that is used for cyclone/hurricane. The simple formats using indices or levels have another merit in observations: it becomes easier to switch to burst-mode monitoring and to make the post-event analyses such as event identification and statistics. For example, ASC image can be taken more frequent (like 5-10 sec resolution) than nominal 1 min resolution during high level period, allowing us to keep archiving size as small as possible.

The question is then (1) how to define and calculate these numbers from the auroral image and also (2) how to derive the activity levels from these numbers. Thus, the task can be divided into two part, with the first part evaluating the contributions from different light sources (e.g., aurora, moon, cloud), and make it as simple but sufficient as possible to evaluate the activity level. A successful result of (1) should make part (2) easy.

For the first part, we use an expert system in which a combination of simple mathematical criteria is applied to each pixel to classify into the difference light sources. This part requires a large computing ability for real-time processing because a large number of input data (each pixel of about 150000 active pixels has a  $256 \times 256 \times 256$  colour values) should be processed simultaneously. Ideally we should judge the neighbouring pixels together to determine the classification of one pixel, but that



requires too much computation resource. Therefore, we judge **each pixel independently** in the present version (ver. 1) except the judgement of the Moon that occupies **solid** small area. For the same reason, we define the level using only the index values but not the each pixels information at all.

Several groups have started identification of aurora or even the classification of aurora using neural network (deep learning) directly from ASC images (e.g., Kvanmmen et al., 2020; Nanjo et al., 2021). The neural network is powerful and rapidly developing tool and even the real time classification is implemented (<https://tromsoe-ai.cei.uec.ac.jp/#/>). However, neural network includes a black box that depends strongly on the learning set, and it might be difficult to identify the reason for any error in the judgement. **Therefore, we take a different approach using sets of solid criteria so that we can identify the reason for any error in the judgement, which is inevitable in improving the algorithm for the future version 2, version 3, etc.**

As the source ASC data, we use **jpeg** images in order to widen the potential **users** of the method to the other cameras, including cameras in domes owned by schools and private sectors (e.g., Toyomasu et al., 2008). With such wide application, a successful judgement of auroral pixels and of auroral activity would benefit not only science (event identification) and operations (archiving, satellite, space weather counterpart), but also education and tourism.

## 2 Algorithm and source data

As mentioned above, there are two major tasks: (1) to obtain the aurora ASC index (a set of numbers) from large information ( $256^3=1.7\times 10^7$  colour values for  $1.5\times 10^5$  pixels each), and (2) to evaluate the activity level from this index. The first task is further subdivided into two steps: (1a) assessment of each pixel using simple mathematical criteria, and (1b) integrate the classification results of all pixels into a simple set of number.

In step (1a), we classify each pixel into different categories such as the aurora (three different levels), cloud, moon, artificial light, and unclassified. The detail is described in section 2.1. In step (1b), these classification and actual values of the colour code (L value) are used to obtain some sort of integrated value, such as numbers of pixels and average luminosity of the most intense auroral pixels, as described in section 2.2. Once the auroral index (set of numbers) is obtained, we evaluate the auroral activity level using only these index values. This is described in section 2.3.

The source data is jpeg images from Kiruna ASC operated by Kiruna Atmospheric and Geophysical Observatory (KAGO) at Swedish Institute of Space Physics. The ASC is located in a 30 cm heated dome at the roof of the optical laboratory in Kiruna at 68 degree north. From September 2020, Kiruna ASC uses Sony  $\alpha 7s$  with a Nikon Nikkor 8 mm 1:2.8 objective lens. The camera is controlled by a Raspberry Pi 4 computer and data is stored on a large disk-server and made available in real time (<https://www.irf.se/sv/observatorieverksamhet/firmamentkamera/>). Data is stored in the **jpeg** format, mainly due to storage space limitations.

The main objective of Kiruna ASC is to overview of the sky with emphasis on Auroral imaging. **The camera is configured for night-time observations and it operates with dynamic exposure time in order to be able to observe during twilight conditions.** The dynamic exposure makes it difficult to define the ASC auroral index, but it is still feasible because we do not have to define one-to-one relation between the colour and category as **long as we can define the activity level properly.**



### RGB 3-D space (256x256x256)

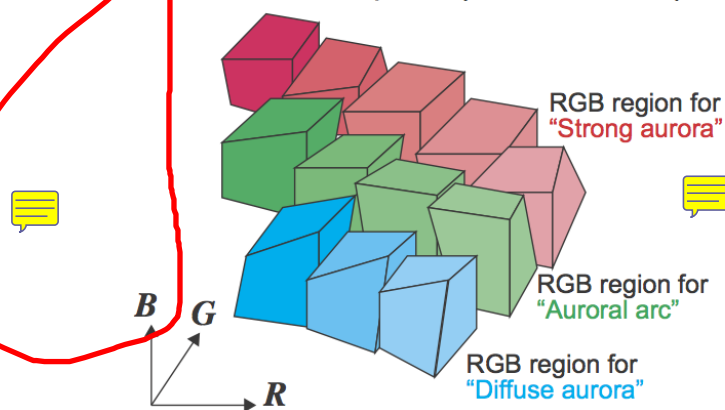


**Figure 1.** Schematic illustration of the criteria of auroral pixel. Each small box with colours represents one criterion that is separated by "or" logic. The criterion are thus restrictive, giving as a room to add more pixels to identify aurora such as pixels dominated by the  $N_2$  red line

## 2.1 Classification of each pixel

95 Standard digital cameras take colour images using three CCDs of wide spectrum coverage centered at red, green, and blue colours, respectively. The values of detected intensity by each CCD composes the RGB colour code. Naturally, green aurora (558 nm) is registered mainly as high G values. However, using only green values (G) is misleading because, in the RGB colour code, all bright pixels like cloud reflection, moon, and artificial light have high G values. The difference between these objects and aurora is seen in the other colours: auroral pixel has a lower intensities in red (R) and/or in blue (B).

100 To extract auroral pixels from pixels with high R values, one solution is to use hue (H) values in hue-saturation-luminosity (HSL) colour code, which can be derived until RGB values. Using HSL colour code, we actually made primitive version (version 0) of a real-time classification for old KAGO's ASC (Nikon D700 camera) from November 2016 and April 2020 (see Appendix A for the criterion). However, the HSL method does not give high enough accuracy in the identification of the auroral pixels, particularly for the SONY camera that is in use from August 2020. To improve the classification accuracy, we  
105 use all R, G, B values to judge each pixel.

The concept is illustrated in Figure 1: we define auroral pixels as summation of many small area in the RGB three dimensional space. The final shape of auroral pixels composes relatively solid areas, which is probably better described by principal component (the criterion becomes very simple in the coordinate system using principal components), and H is a good candidate for one of such component. However, after examining individual pixels, we found that H criterion fluctuates depending on the  
110 auroral luminosity and on the effects of moon, cloud, and artificial light.

Here, we also note that we can accept small errors in the ASC auroral index because ~~we~~ our final goal is to obtain the activity level. Furthermore, values (0-255) for R, G, B can take only limited discrete numbers. Therefore, we can accept some uncertainly in judging each pixel in terms of different categories when performing. In other words, we do not have to define



**Table 1.** Criteria of pixels for category "strong aurora" (one of them)

classification	condition 1	condition 2	condition 3	condition 4	condition 5
arc mix with N <sub>2</sub> red line 1a:	$0.25 \leq H < 0.34$	$0.97 \leq G$	$0.50 \leq R/G < 0.92$		$(R+B)/G < 1.90$
arc mix with N <sub>2</sub> red line 1b:	$0.25 \leq H < 0.34$	$0.995 \leq G$	$0.50 \leq R/G < 0.95$		$(R+B)/G < 1.90$
strong green arc 1:	$0.26 \leq H < 0.36$	$0.95 \leq G$	$R/G < 0.75$		$(R+B)/G < 1.90$
strong green arc 2:	$0.30 \leq H < 0.36$	$0.88 \leq G$	$R/G < 0.70$	$B/G < 0.66$	
strong green arc 3:	$0.30 \leq H < 0.34$	$0.83 \leq G$	$R/G < 0.62$	$B/G < 0.57$	
strong green arc 4:	$0.32 \leq H < 0.36$	$0.76 \leq G$	$R/G < 0.43$	$B/G < 0.50$	$(R+B)/G < 0.89$
strong green arc 5:	$0.30 \leq H < 0.352$	$0.77 \leq G < 0.83$	$R/G < 0.60$	$B/G < 0.64$	$(R+B)/G \geq 0.96$
strong green arc 6:	$0.26 \leq H < 0.31$	$0.75 \leq G < 0.95$	$R/G < 0.69$	$B/G < 0.54$	

one-to-one relation between the colour of the pixel and classification category. With these limitations, a manual definition  
 115 of many small RGB-space like Figure 1 is not very much different from ideal criterion including those using the principal  
 component method.

For aurora, we define three categories: most likely "strong aurora" (Table 1), "green arc" that is most likely discrete aurora  
 (Table 2), and "visible diffuse" that is most likely strong diffuse aurora (Table 3), respectively. Here, strong aurora means  
 either the intensity is very high, like intensified arc during substorms causing saturation of the R value (while other values also  
 120 increases with absolute intensity), or like the arc mixed with N<sub>2</sub> red line (670 nm). Either of them causes the colour closer  
 to white, but we limit the definition of strong aurora to those in which the green colour is dominant, i.e., G is larger than R  
 and B (this is equivalent to  $0.167 \leq H < 0.5$ ). We also apply the same limitation (the green colour dominance) to the other two  
 auroral categories. In other words, pixels that are dominated by the N<sub>2</sub> red line with  $R > G$  are excluded in the present version  
 (considering these N<sub>2</sub>-dominant pixels is one of the future tasks).

125 Having three categories instead of two (discrete and diffuse) has an advantage because the actual classification is fuzzy  
 and often difficult to judge between discrete and diffuse. By having three categories, we can define "strong aurora" as clearly  
 discrete one. Similarly, we dismissed weak diffuse aurora as "dark" because that is not very important for the level definition.  
 Otherwise the definition is exclusive, i.e., auroral that does not meet these criteria are not included as aurora. Such a false-  
 positive case happens when the aurora is through the cloud or under effect of artificial light.

130 The advantage of the exclusive definition is that we can add new criterion by adding "or" criterion, in case we miss some  
 type of aurora in the present criterion. For example, strong N<sub>2</sub> red line with very little green line can be added after separating  
 its colour code from the twilight. So far, we have not included such strong N<sub>2</sub> red line pixels as the aurora pixels because such  
 an aurora is normally accompanied by the "strong aurora" on the same image or images 1 minutes before or after, and does not  
 affect the final judgement of the auroral activity very much.

135 Table 4 shows criterions for "artificial light", Table 5 for "cloud" without aurora, Table 6 for "cloud" but possibly under  
 aurora, and Table 7 for "moon" and its surroundings. Here, the moon body is obtained from the image as a densely populated



**Table 2.** Criteria of pixels for category "green arc" (one of them)

classification	condition 1	condition 2	condition 3	condition 4	condition 5
green arc 1:	$0.32 \leq H < 0.36$	$0.69 \leq G$	$R/G < 0.47$	$B/G < 0.51$	
green arc 2:	$0.36 \leq H < 0.41$	$0.69 \leq G$	$R/G < 0.70$	$B/G < 0.80$	
green arc 3a:	$0.28 \leq H < 0.35$	$0.65 \leq G < 0.80$	$R/G < 0.70$		$(R+B)/G < 1.21$
green arc 3b:	$0.28 \leq H < 0.35$	$0.65 \leq G < 0.80$	$R/G < 0.70$	$B/G < 0.62$	
green arc 4:	$0.24 \leq H < 0.27$	$0.59 \leq G < 0.70$	$R/G < 0.80$	$B/G < 0.55$	
green arc 5:	$0.20 \leq H < 0.24$	$0.59 \leq G < 0.77$	$R/G < 0.92$	$B/G < 0.65$	
green arc 6:	$0.30 \leq H < 0.36$	$0.55 \leq G < 0.68$	$R/G < 0.61$	$B/G < 0.61$	
green arc 7:	$0.25 \leq H < 0.35$	$0.50 \leq G < 0.69$	$R/G < 0.75$	$B/G < 0.51$	

**Table 3.** Criteria of pixels for category "visible diffuse" (one of them)

classification	condition 1	condition 2	condition 3	condition 4	condition 5	condition 6
light contaminated 1:	$0.31 \leq H < 0.38$	$0.85 \leq G < 0.94$	$R/G < 0.92$	$B/G < 0.93$	$(R+B)/G < 1.83$	
light contaminated 2:	$0.36 \leq H < 0.43$	$0.61 \leq G < 0.80$	$R/G < 0.88$	$B/G < 0.92$	$(R+B)/G < 1.70$	
strong diffuse or arc:	$0.24 \leq H < 0.31$	$0.40 \leq G < 0.80$	$R/G < 0.72$	$B/G < 0.40$		
diffuse or weak arc 1:	$0.30 \leq H < 0.36$	$0.61 \leq G < 0.87$	$R/G < 0.83$	$B/G < 0.80$	$(R+B)/G < 1.60$	
diffuse or weak arc 2:	$0.33 \leq H < 0.38$	$0.40 \leq G < 0.65$	$R/G < 0.87$	$B/G < 0.90$	$(R+B)/G < 1.70$	$R+G+B > 0.98$
diffuse or weak arc 3:	$0.40 \leq H < 0.47$	$0.40 \leq G < 0.65$	$R/G < 0.72$	$B/G < 0.96$	$(R+B)/G < 1.60$	$R+G+B > 0.98$
arc through cloud:	$0.19 \leq H < 0.21$	$0.56 \leq G < 0.75$	$R/G < 0.95$	$B/G < 0.6$		

solid region of pixels that satisfy the moon criterion. We decided not to use the moon location calculated from the time and the orbit because the moon location is deformed by the dome, and the moon is often hidden by the cloud.

In these classifications, some pixels meet two or more different definitions. Therefore, we also give a priority order in the following: 1. artificial light (Table 4) and the moon (Table 7), 2. strong aurora (Table 1), 3. green arc (Table 2), 4. visible aurora (Table 3), and 5. cloud (Tables 5 and 6). This means that we may miss some of the aurora pixels, particularly very strong one (e.g.,  $G=1.0$ ) is identified as "green arc" or "strong aurora", as long as  $0.24 < H < 0.34$

The underestimation of auroral pixel due to the saturation is not a problem because what we need is approximate coverage of auroral coverage with 0.05-0.1% accuracy, i.e., about 100 pixels out of  $1.5 \times 10^5$  pixels, and because the major error comes from the fact that a large part of the sky is covered by the cloud and the moon. Because of large number of pixels, we do not need exact one-to-one relation between the aurora and classification category.



**Table 4.** Criterions of city light pixels (one of them)

classification	condition 1	condition 2	condition 3	condition 4	condition 5
city light 1:	$0.45 \leq H < 0.67$	$0.65 \leq G < 0.92$	$0.91 \leq R/G < 1.01$	$0.92 \leq B/G < 1.05$	
city light 2:	$0.39 \leq H < 0.50$	$0.66 \leq G < 0.74$	$0.88 \leq R/G < 0.94$	$0.92 \leq B/G < 1.00$	$1.82 \leq (R+B)/G$
city light 3:	$0.15 \leq H < 0.19$	$0.66 \leq G < 0.74$	$0.94 \leq R/G < 1.01$	$0.96 \leq B/G < 1.00$	
diffuse+light:	$0.26 \leq H < 0.46$	$0.71 \leq G < 0.92$	$0.91 \leq R/G < 0.98$	$0.92 \leq B/G < 0.99$	

**Table 5.** Criterions of cloud pixels when no aurora appear (one of them)

classification	condition 1	condition 2	condition 3	condition 4	condition 5	condition 6
cloud w town light 1:		$0.995 \leq G$	$0.995 \leq R$	$0.92 \leq B/G$	$B < G - 0.018$	$B < R - 0.018$
cloud w town light 2:	$0.10 \leq H < 0.24$	$0.94 \leq G < 0.995$	$0.99 \leq R$	$0.89 \leq B/G$	$B < G - 0.018$	
cloud w town light 3:	$0.10 \leq H < 0.19$	$0.60 \leq G < 0.96$	$0.97 \leq R/G < 1.10$	$0.65 \leq B/G < 0.90$		
cloud near moon:	$0.18 \leq H < 0.27$	$0.64 \leq G < 0.77$	$0.92 \leq R/G < 1.00$	$0.86 \leq B/G < 0.96$		
cloud (less blight) 4:	$0.10 \leq H < 0.20$	$0.50 \leq G < 0.67$	$0.95 \leq R/G$	$0.55 \leq B/G < 0.80$	$1.52 \leq (R+B)/G$	
cloud (less blight) 5:	$0.12 \leq H < 0.20$	$0.38 \leq G < 0.55$	$0.92 \leq R/G$	$0.50 \leq B/G < 0.70$	$1.49 \leq (R+B)/G$	
cloud reflects aurora:	$0.17 \leq H < 0.29$	$0.41 \leq G < 0.60$	$0.65 \leq R/G$	$0.50 \leq B/G$		$B < R - 0.10$

Another problem is that the moon modifies the colour at almost all pixels due to the refraction at the dome. The auroral colour is modified toward higher L values by the moon even if the auroral pixel is far away from the moon. This modification is larger at closer pixels to the moon. In addition, the moon modifies the H values (B-G-R ratio) in the actual observations as shown in the examples in Section 3.

To reduce the moon effect, a certain distance from the moon pixels are masked. This causes underestimation of numbers of pixels of the strong aurora within this masking distance, although eye identification can judge these strong auroral pixels. Such a coincidence actually happens because the moon is normally located in the south at which the Local-Arc-Breaking sometimes takes place for the Kiruna ASC. Fortunately, after five months of operation, number of the missed Local-Arc-Breaking due to this coincident is small because the aurora often expands beyond the masked region after the Local-Arc-Breaking. We anyway plan to improve this in the future, but the present version of dealing with the moon is still effective.

We imposed another mask in the northwest edge where both the artificial green light source and strong city light is within the field of view. Since the light source covers only near the edge, we simply remove the entire section from the analyses.



**Table 6.** Criteria of cloud pixels most likely under aurora (one of them)

classification	condition 1	condition 2	condition 3	condition 4
cloud under diffuse 8:	$0.26 \leq H < 0.32$	$0.60 \leq G < 0.70$	$0.90 \leq R/G < 0.97$	$0.88 \leq B/G$
cloud under diffuse 9:	$0.47 \leq H < 0.55$	$0.55 \leq G < 0.70$	$0.80 \leq R/G < 0.95$	$0.95 \leq B/G$

**Table 7.** Criteria of moon pixels (one of them)

classification	condition 1	condition 2	condition 3	condition 4	condition 5
moon center:	$0.995 \leq G$	$0.995 \leq R$	$G - 0.024 \leq B$	$B < G + 0.005$	
moon core:	$0.95 \leq G < 0.997$	$G - 0.005 \leq R < G + 0.017$		$B/G \leq 1.00$	$1.95 \leq (R+B)/G < 2.01$
surrounding:	$0.70 \leq G < 0.97$	$0.994 \leq R/G < 1.024$	$0.93 < B/G$	$B/G < 0.98$	
affected:	$0.60 \leq G < 0.90$	$0.79 \leq R/G < 0.98$	$0.94 \leq B/G$	$B < G - 0.005$	$0.42 \leq H < 0.50$

## 160 2.2 Calculation of the aurora ASC index

Now we have classification scheme for each pixel (Tables 1-7). We next obtain a simple set of numbers (parameters) representing all pixels. The obvious parameter is the numbers of pixel, or more precisely, percentage of the coverage over the sky. The "strong aurora" (which means saturation with the  $N_2$  red lines) is normally identified at a small part of the sky even during very active time, ranging normally around 0.1-5% during and before the Local-Arc-Breaking. Therefore, an accuracy of 0.03% in numbers of pixels (about 50 pixels) is sufficient to judge the activity level. For the arc aurora that occupies a larger area (normally around 1-20% during and before the Local-Arc-Breaking), 0.1% accuracy in numbers of pixels (about 150 pixels) is sufficient to judge the activity level. Any digit better than these numbers is just noise in the present case. Therefore, we obtain the coverage of aurora with accuracy of 0.01% for "strong aurora" and 0.1% for the "green arc" and "visible diffuse". For the other non-auroral categories, our identification accuracy is not better than 1%, but still we obtain 0.1% accuracy when deriving the number.

The simple percentage of the auroral pixels over the sky, however, is not sufficient because it gives higher values for relatively less luminous aurora with wide area than relatively more luminous aurora with small area within the same category. Another problem is that the brightness given as L values is not proportional to the numbers of auroral intensity counted by numbers of photons (Sigernes et al., 2014). Therefore, we also obtain "characteristic brightness" of the aurora. Here, we do not take a simple summation of the luminosity values (L in the HSL colour code, that is  $L = (R+G+B)/3$ ), because such a summation still gives higher values for wide aurora with low L values than compact aurora with high L values. Instead, we obtain a kind of average intensity of the "strong aurora" pixels, as described below.





**Table 8.** Content of ASC auroral index

Index content	explanation
%diffuse	occupancy (in %) of visible diffuse pixels
%arc	occupancy (in %) of green arc pixels
%strong	occupancy (in %) of strong aurora pixels (either saturated or N <sub>2</sub> red line is contaminated to the green aurora)
%void	occupancy (in %) of void pixels due to the moon light, artificial light, and obvious cloud that reflects the artificial light
%cloud	occupancy (in %) of specifically the cloud pixels. Note that this is significantly underestimated.
L1	corrected average <L> (luminosity in the HSL) after nonlinear weighting by %arc (and %strong for very small %strong)
L3	corrected average <L <sup>3</sup> > after nonlinear weighting by %arc (and %strong for very small %strong)

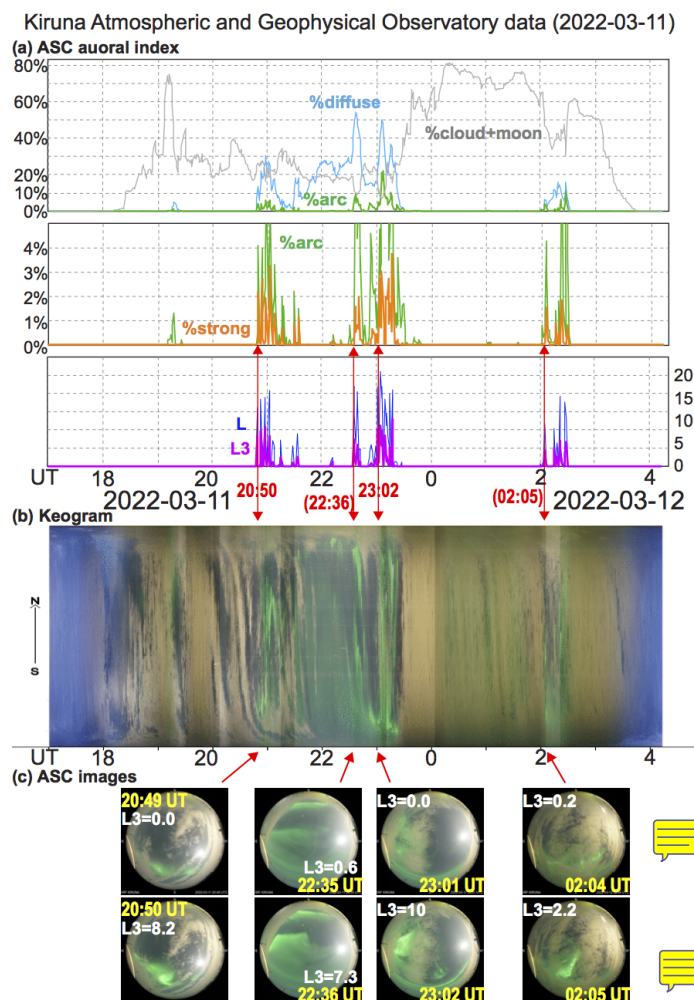
If the number of pixels of the "strong aurora" exceeds 4900 pixels (about about 3% of the image), we simply use the pixel data for the most luminous 4900 pixels (judged by the L value) among the "strong aurora" pixels. Afterward, we use a nonlinear schemes for averaging. We first take the average of both L values and L<sup>3</sup> values. We reduce the obtained average values if the numbers of auroral pixels are small with the coefficient roughly proportional to  $1/\sqrt{n_{arc}}$ , where  $n_{arc}$  is number of pixel of "green arc", and zero when "strong aurora" pixels are less than 10. Here we use L value as representing the luminosity, but we can use G values because what we are counting is intensity of the green (558 nm) aurora. The exact python code is found in the supplemental material.

Table 8 summarizes the obtained parameters for the ASC auroral index. The obtained values are stored in an ascii format as a csv file on a website in real-time every minutes (<https://www.irf.se/alis/allsky/nowcast/>). The real-time plot and the archive of the past data are also found on the same website. For the ascii file, we temporally made its width only 72 columns without tab, which makes the file format very similar to the IAGA2002 format of the geomagnetic field. It is quite possible to extend the column to include other key parameter such as moon position and auroral position, but that will be a future task.

Figure 2 shows an example of comparison between the index values and the keogram over one night (11-12 March 2022). ASC images when the Level 6 activity is detected was also displayed at the bottom One can see good correspondence with the index values and keogram image. However, we should note that the present calculations and criterions are valid only for Kiruna ASC because the classification criterions are different at different location (city light and latitude). For example, cloud identification by Sodium line (589 nm) is specific for Kiruna ASC because of strong light-pollution by the city light. This makes identification of cloud relatively simple but identification of weak aurora relatively difficult (the hue values are next to each other).

### 2.3 Evaluation of the activity level from the aurora ASC index

The next task is to evaluate the activity level and particularly define the criterion that correspond to the Local-Arc-Breaking (sudden and significant intensification of auroral arc with expanding motion), from these index values without examining the



**Figure 2.** An example of (a) ASC auroral index over one night with both active aurora and occasional cloud 11-12 March, 2022. As reference, (b) keogram over the same night and (c) all-sky images at the time of auroral alert are issued for Level 6 activities. Each image is taken toward the sky with north in the top, and hence east (west) is left (right). The automatic exposure time is 4s or 5s for the displayed images.

200 image data. The significant intensity means high values of L1 or L3, and expansion means more than certain values of "%arc" and "% strong". Table 9 summarizes the criteria for the activity level (Level 6) that most likely corresponds to the Local-Arc-Breaking in the Kiruna ASC. We also defined Level 4a and Level 4b for auroral activity that is close to but less intense than Level 6, as possible candidates for a precursor of the Local-Arc-Breaking.

205 Once Level 6 is detected in the real-time ASC image, an alert is sent to the registered mail addresses. We started this alerting system from 5th November, 2021. Due to many cloudy nights (particularly during November and December), Level 6 was detected in limited numbers of nights, but still sufficient to validate this method. In this validation, we examined all ASC images by eye (traditional method), and therefore, judgement of the Local-Arc-Breaking is somewhat subjective. However,



**Table 9.** Criteria for the activity level

Level	condition 1	condition 2	condition 3
Level 6:	%arc $\geq$ 3% (eventually $\geq$ 2.95%)	%strong $\geq$ 0.2% (eventually $\geq$ 0.195%)	L3 $\geq$ 8 (eventually $\geq$ 7.95)
Level 4a:	%arc $\geq$ 2% (eventually $\geq$ 1.95%)	%strong $\geq$ 0.2% (eventually $\geq$ 0.195%)	L3 $\geq$ 5 (eventually $\geq$ 4.95)
Level 4b:	%arc $\geq$ 1% (eventually $\geq$ 0.95%)	%strong $\geq$ 0.1% (eventually $\geq$ 0.095%)	%strong·L3 $\geq$ 1.5%

**Table 10.** List of Level 6 alert during 5 November 2021 - 12 April 2022

month	day
November 2021:	6, 8, 9, 15, [19=moon (L3=0)] <sup>*1,*2</sup> , 20, [23=N] <sup>*3</sup>
December 2021:	5, 6, 19, 21, 27, 31
January 2022:	1, 8, 9, 14, 15, 18, [19=moon (L3=6.9)], 21, 22, 24, 25, 27, 28, 30, 31
February 2022 <sup>*4</sup> :	[8=N], 10, 11, 12, 13,
March 2022:	1, 3, 5, 6, [7=N], 8, 9, 10, 11, [12=N], 13, [15=moon (L3=7.8)], 19, 20, 21, 22, 23, 26
April 2022:	[3=dusk] <sup>*5</sup> , 7, 12, [14=dusk]

\*1: Bracket [] indicates that the Local-Arc-Breaking was seen in the image without Level 6 alert.

\*2: "=moon" indicates relatively weak intensification such that moon contamination prevented the identification "strong aurora".

\*3: "=N" indicates breaking up in the northern sky and not covering the zenith, such that numbers of "strong aurora" did not reach the criterion.

\*4: auroral camera was not running on 16-19, and 21 February (total 5 nights).

\*5: "=dusk" indicates relatively weak breaking up in the dusk sky with some sunlight effect remains, such that exposure time too short to recognize sufficient numbers of auroral pixels.

considering its purpose of event identification and real-time warning, both of which also rely on subjective definition, the eye-identification method is sufficient for the validation for the Level 6 definition.

210 Table 10 summarizes the validation result (Level 6 is detected or not over one night). The table lists the night when Level 6 is detected for each month from 5 November, 2021 to 14 April, 2022. Note that twilight effect makes the detection of Level 6 very difficult already from 3 April, and impossible to detect from 14 April. The date inside the bracket indicates that the Local-Arc-Breaking was seen in the ASC images without reaching Level 6 (except possible Local-Arc-Breaking in very north because it is difficult to judge). Unless the aurora brightening takes place very north, above the cloud, or hidden by the moon, 215 the eye-identified auroral brightening is well represented by Level 6 within ten minutes offset.

### 3 Examples

In this section we show examples of ASC auroral index and ASC images around Local-Arc-Breaking.



### 3.1 Successful cases

220 First Level 6 activity after we started the automated mail alert was detected on 6 November 2021, day after we started the system (cloudy on 5 November). Figure 3 shows the series of Kiruna ASC images around the first Level 6 detection on that day. The ASC auroral index values are given at the bottom of each images. In addition, cloud coverage (in %) is given at the top of each image in Figure 3 (but not other figures with ASC images). Each image is taken toward the sky with north in the top, and hence east (west) is left (right).

225 In Figure 3, the Local-Arc-Breaking (most likely the arrival of the auroral substorm bulge to this local time) is seen at 17:31 UT (around 20 MLT) and simultaneously Level 6 is detected for the first time in this evening. Before this Local-Arc-Breaking, intensification of the auroral arc equatorward of the original arc was recognised at 17:27 UT. In this example, two of three Level 6 conditions,  $\%arc \geq 3\%$  and  $\%strong \geq 0.2\%$ , are satisfied from already 17:18 UT, as shown in Figure 4a, and  $L3 \geq 8$  is the condition that demarcates the activity Level. . As a reference, we also show the geomagnetic variation during this period in Figures 4b and 4c. Figure 4b shows fluxgate (DC) magnetometer data and Figure 4c shows its variation that is represented  
230 by three different methods: two  $|dB/dt|$  values using 1s resolution data and 10s-running average (still 1s resolution) data, respectively, and the standard deviation divided by square root of 60s ( $\sim 7.75s^{0.5}$ ), i.e., normalized fluctuation over 60s. At 17:31 UT when the auroral brightening reached to Level 6, the geomagnetic field suddenly changed, with  $B_x$  started changing by more than 100 nT within a minute (this satisfies necessary condition of a substorm) while magnetic deviation increased by an order of magnitude in all three methods.

235 The next detection of Level 6 activity was under more cloudy condition at 20:43 UT (around 23 MLT) on the same day. Figure 5 shows the series of Kiruna ASC images, time series plots of the ASC auroral index values and geomagnetic activities in the same format as Figures 3 and 4. Due to high cloud coverage (almost full coverage over the sky), auroral arc before the sudden and significant intensification was not well recognised until one minute before (20:42 UT), at which only one parameter ( $\%arc$ ) reached the criterion of Level 6, while other parameters ( $\%strong$  and  $L3$ ) did not reach the criterion of Level 4a or 4b.  
240 Fortunately the cloud was not very thick and the brightening aurora was strong enough to be recognized in the ASC auroral index through the cloud. The timing of Level 6 detection (20:43 UT) again corresponds to large geomagnetic deviation with more than 100 nT change in  $B_x$  and nearly one order of magnitude increase of the magnetic deviation in all three methods.

In both examples (17:31 UT and 20:43 UT), Level 6 detection timing agrees with the timing of the Local-Arc-Breaking in the ASC image, and the morphology the Local-Arc-Breaking is consistent with the evening auroral surge during a substorm  
245 (Akasofu, 1964). The last detection of the Level 6 activity on the same night took place in the post-midnight sector at 23:15 UT (around 01 MLT, i.e., post-midnight). Figure 6 shows the relevant images and plots in the same format as Figure 5. In this example, the aurora brightening started already at 23:13 UT, two minutes before the Level 6 detection, as is also indicated by the geomagnetic deviation (90 nT change of the X component in 2 minutes). Instead of Level 6, ASC auroral index values gave Level 4b at 23:13 UT, and Level 4a at 23:14 UT. The magnetic deviation also increased significantly, but the peak values are  
250 much lower than previous Level 6 activities (Figures 4 and 5) by more than a factor of 3. Considering such a small geomagnetic activity, two minutes delay of Level 6 detection is still successful for the real-time alert.

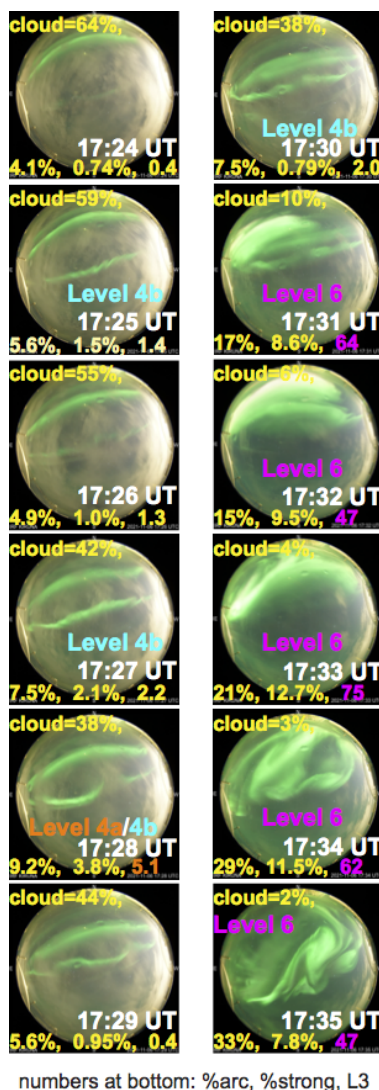


**Figure 3.** ASC images around 17:31 UT on 6 November 2021, when the first Level 6 was detected after we started the real-time Level 6 alert by E-mail. The north in the top, and east (west) is left (right). The ASC index values are given at the bottom of each images. The timing of Level 6 detection is the same as the onset of the Local-Arc-Breaking. The automatic exposure time (8s at 17:31 UT) is much longer than those of Figure 2c (4s-5s).

We should note, however, that the relation between the index values and auroral activities are generally different between the pre-midnight and post-midnight because the auroral morphology is different between them (e.g., Akasofu, 1964). For example, diffuse aurora in the post-midnight is often registered as "green arc". Therefore, we need to make different criterions between  
 255 pre-midnight and post-midnight in the future. On the other hand, the judgement of Level 6 is not very much affected by this

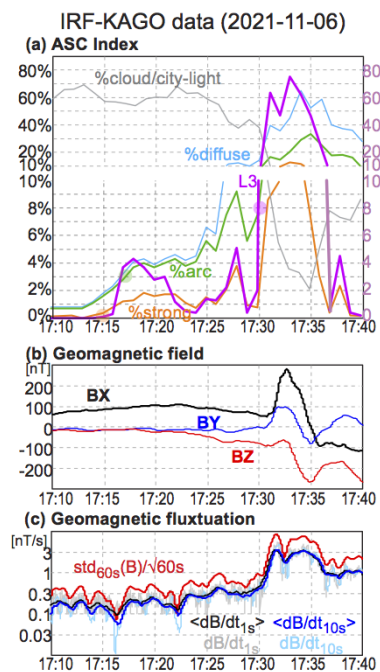


**Figure 4.** Time series of the ASC auroral index values and geomagnetic data during 17:10-17:40 including the period of Figure 3, i.e., around the first Level-6 detection at 17:31 UT on 6 November 2021. (a) ASC index values. (b) DC geomagnetic deviation from the baseline values (X=north, Y=east, Z=downward). (c) AC geomagnetic variation measured by  $|dB/dt|$  using 1-sec values (black), and using 10 sec running average values (blue), respectively, and standard deviation of magnetic field over 60 sec using 1-sec values and normalised to nT/s unit (red). These variations are first calculated for each vector component, and then taken the absolute values.

because the criterion the L3 value is not very much affected. This is why we keep the consideration of the local time as a future task but not very urgent.

### 3.2 Moon effect

Here, we show two examples with strong influence by the moon: one successful case (15 November 2021, 20:36 UT) in  
 260 Figure 7 and one unsuccessful case (19 January 2022, 23:56 UT) in Figure 8. In the successful case, Level 6 was detected at 20:36 UT, which is only a few minutes after the Local-Arc-Breaking becomes clear in the ASC. For this event, the brightened aurora is located very close to the moon, and that caused relatively low L3 values and low %strong values. Nevertheless, the ASC auroral index values reached to Level 6 Comparing to the local magnetometer data (Figures 7c and 7d) that indicate the Local-Arc-Breaking at 20:39 UT, the ASC index gave closer time to the Local-Arc-Breaking.

265 In the unsuccessful case (Figure 8), the peak L3 value was only 6.9 at 23:57 UT although the ASC image shows the Local-Arc-Breaking some distance north from the moon. The geomagnetic deviation (Figure 8c)  $> 150$  nT changes in 5 minutes and magnetic variation (Figure 8d) also reached the level of Local-Arc-Breaking in the previous examples. Both %arc (=7.0%) and



Kiruna Atmospheric and Geophysical Observatory data (2021-11-06)

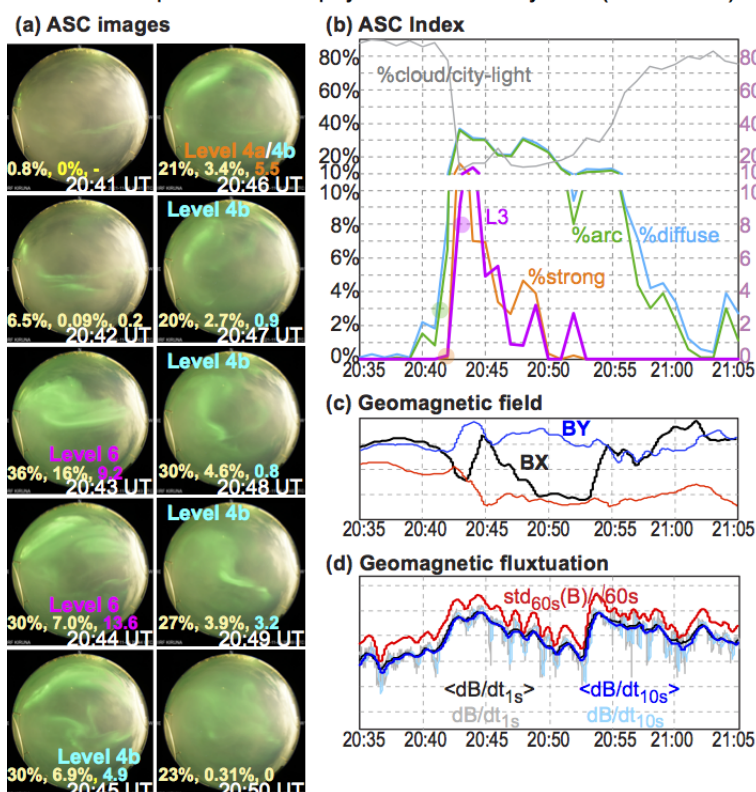


**Figure 5.** ASC images, the ASC auroral index values and geomagnetic data around the time when the Level 6 aurora activity was detected at 20:43 UT on 6 November, 2021. The format is the same of combination of Figures 3 and 4 except that the cloud coverage is not shown on the ASC images. The automatic exposure time (5s at 20:43 UT) is similar to those of Figure 2c (4s-5s).

270 %strong (=0.41%) exceeded the Level 6 criterion at this time, clearing both Level 4a and Level 4b. Thus, only the L3 value did not reach the Level 6 criterion. The small L3 value might also have come from the change of the colour: background (night sky) colour in the ASC images is more bluish than the ASC images on 6 November, 2021. This change is probably due to the wide refraction of moonlight through the dome. By adding blue colour, the criterion of the "strong aurora" is affected. Taking care of this problem is one of the future tasks. One may also attribute a short exposure time (2s) that is only the half of the successful case in Figure 7a (4s), but it is not clear how much it affects to the ASC auroral index, according to the examination of the twilight case in Figure 9.

275 **3.3 Twilight effect in spring and fall**

Like the moon effect case, twilight case also changes the colour of the entire image toward blue. Figure 9 shows one such unsuccessful case. A clear Local-Arc-Breaking took place in the northern sky. In fact the L3 value exceeded the Level 6

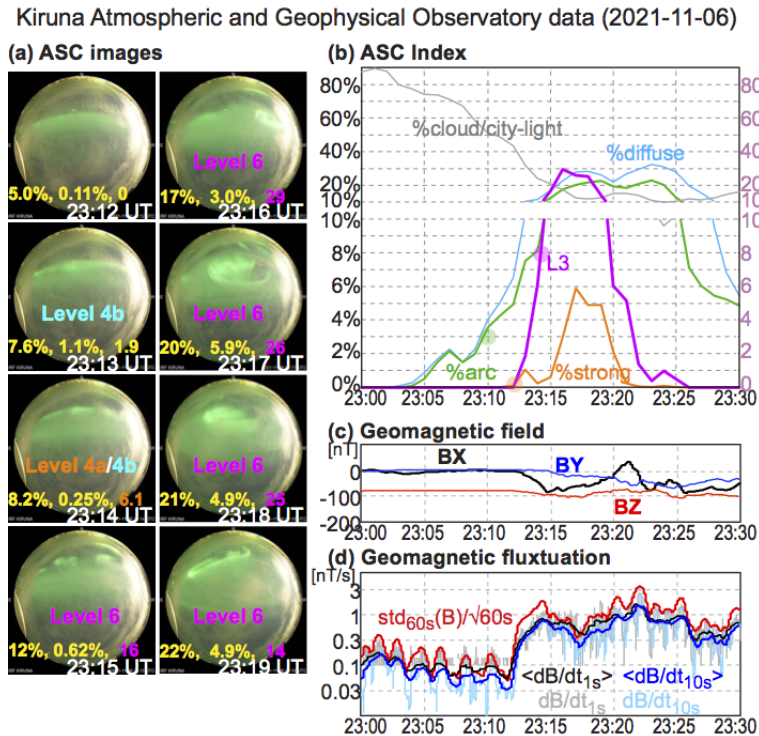


**Figure 6.** The same as Figure 5 for the Level 6 auroral activity at 23:15 UT on 6 November, 2021. The automatic exposure time (8s at 23:15 UT) is much longer than those of Figure 2c (4s-5s).

280 criterion at 20:06 UT and 20:07 UT. However, the auroral coverage did not reach the needed values (marked by blue circle in Figure 10a), although the exposure time is 4s, which is same or similar to those successful cases in Figure 2, Figure 5, and Figure 7 with %strong values exceeded much beyond the Level 6 criterion. In other words, the short exposure time alone does not prevent the ASC index reaching to Level 6, and therefore we consider the additional blue colour in both the moon case and twilight case might make the auroral pixel more difficult to be identified as "strong aurora".

### 3.4 Missed case due to northward auroral location

285 If the Local-Arc-Breaking takes place in the northern sky, the coverage of the aurora (%arc and %strong) becomes small due to oblique looking angle (marked by blue circle in Figure 9a). This sometimes prevents aurora coverage from satisfying the Level 6 criterion ( $\%arc \geq 3\%$  and  $\%strong \geq 0.2\%$ ), particularly or relatively weak Local-Arc-Breaking. Figure 9 shows one such example breaking up in the far-north (23 November 2021, 21:28UT) without reaching Level 6 due to too small auroral coverage. In this example, a thin cloud reduced the moon light, and hence the reduction of the exposure time is not as significant as the previous cases (Figures 7 and 8). The most blight image was taken at 21:29 UT with sufficient %strong (=1.15%) and L3 (=9.5) for Level 6, but %arc (=1.9%) was far below the required threshold ( $\geq 3\%$ ) for Level 6. The geomagnetic deviation

290



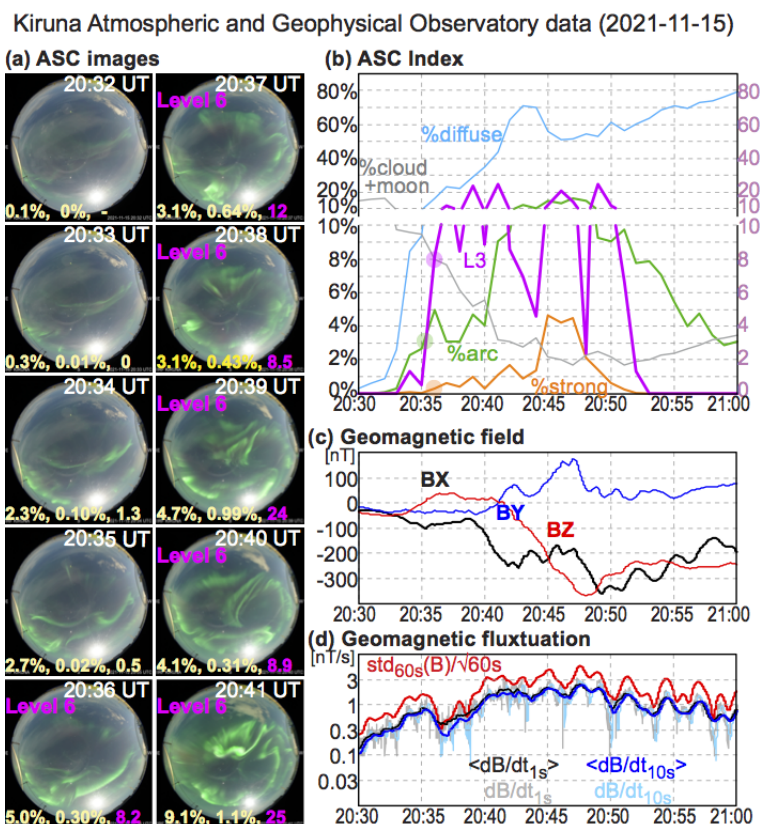


**Figure 7.** The same as Figure 5 for the Level 6 auroral activity at 20:36 UT on 15 November, 2021. The automatic exposure time (4s at 20:36 UT) is similar to those of Figure 2c (4s-5s).

(Figure 9c) of deviation is more than 100 nT with gradual change, and geomagnetic variation (Figure 9d) of about 1-3 nT/s are, considering aurora location far north, large enough to be a Local-Arc-Breaking.

#### 4 Discussion and future tasks

We used three categories of aurora instead of two (discrete aurora and diffuse aurora). Adding a third category between two different phenomena a common method in practical classification of data when the criterion is not very much discrete (i.e., somewhat fizzy). Since our aim is to identify the intensification of aurora rather than aurora itself, adding a third fuzzy category between the discrete aurora and diffuse aurora is even more useful. For the same reason, one may add a new category of "could be aurora" that does not reach the criterion of "visible diffuse" if the purpose is just to identify images that may contain visible aurora. The last one is particularly useful for automated removal of ASC image from the archive (with the condition of no aurora and high cloud coverage).

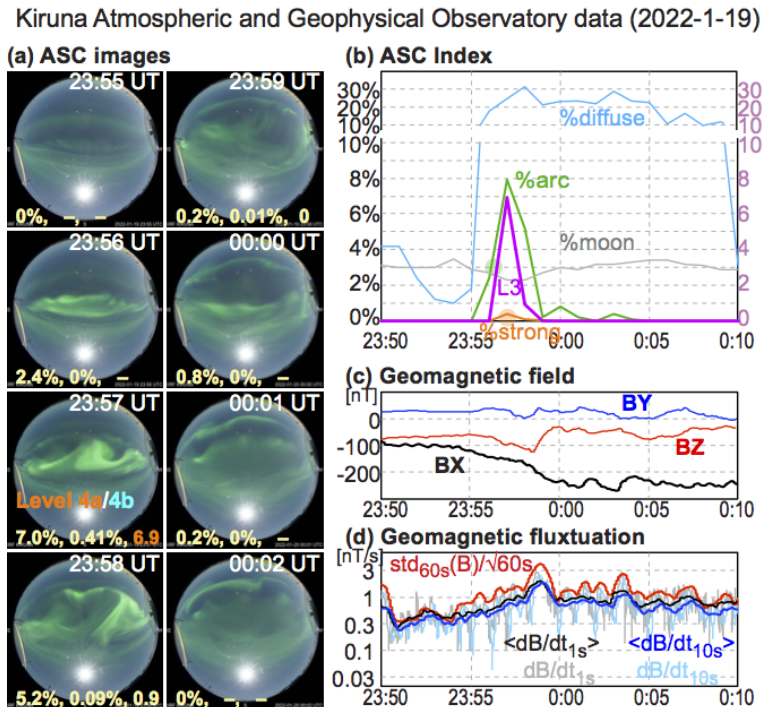


**Figure 8.** The same as Figure 5 for the Level 4a/4b auroral activity at 23:57 UT on 19 January, 2022. The automatic exposure time is shortened to 2s instead of 4s of the previous moon case.

Table 10 lists date that Level 6 was detected. Almost all detection are accompanied by the Local-Arc-Breaking within 10 min, with most of the false negative (detection of Level 6 without Local-Arc-Breaking within 10 min) during intensification of auroral arcs before Local-Arc-Breaking or during the expanded auroral activity (like substorm expansion phase), and are related to the same series of aurora activity related to the Local-Arc-Breaking. Only small fraction of such intensification was not associated with substantial expansion of the aurora (about 10%).

Likewise, false positive is very small, i.e., Level 6 auroral activity was not detected only 9 nights nearly 50 nights with the Local-Arc-Breaking in the ASC. After removing the Local-Arc-Breaking that is affected by moon or twilight, this ratio decrease to 4 night out of about 45 night. Even if we count individual Local-Arc-Breaking when multiple event takes place in one night, this low false rate does not change very much. Thus, the Level 6 definition, although this is just version 1.0, works as the event identification purpose for both realtime campaign and statistical studies.

There are many rooms for future improvement. One advantage using simple criterions is that it is relatively easier to pinpoint the reason why the false warning (Level 6) is issued compared to neural networks (or other black-box method). For example, the mid-term product of each category in the first step (derivation of the ASC auroral index) is stored as a filter matrix of  $\sim 150000$  pixels with true and false values for each category. Therefore, one can examine pixel by pixel in any case of categorizing wrong. This method is actually used to separate the cloud effect during the development of the criterions (Tables 1-7). In addition, we



### KAGO ASC images (2022-4-03)

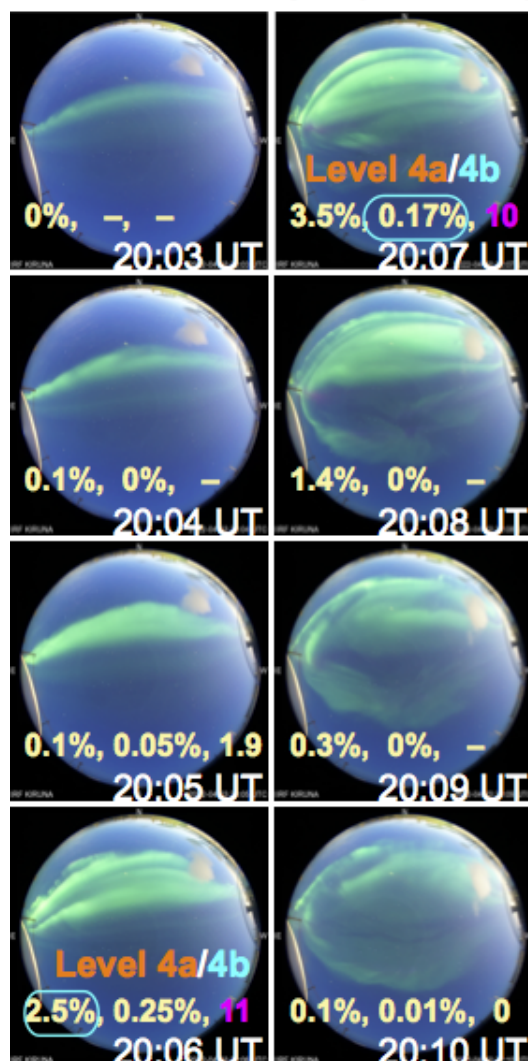


**Figure 9.** ASC images around 20:06 UT on 3 April 2022, when the ASC auroral index values did not reach Level 6 due to the twilight effect when the Local-Arc-Breaking took place. The automatic exposure time is 4s and is the same as those of the successful moon case (Figure 7a) and similar to those of Figure 2c and 5a.

have already identified the reason for the false positive for the moon cases: due to the colour of all pixels becoming bluish. This is due to refraction through the all sky dome, and one possible improvement is, in addition to masking, correct B values by reducing some percentage. The goal is to make the similar values of the ASC auroral index for the same level of aurora between with and without the moon.

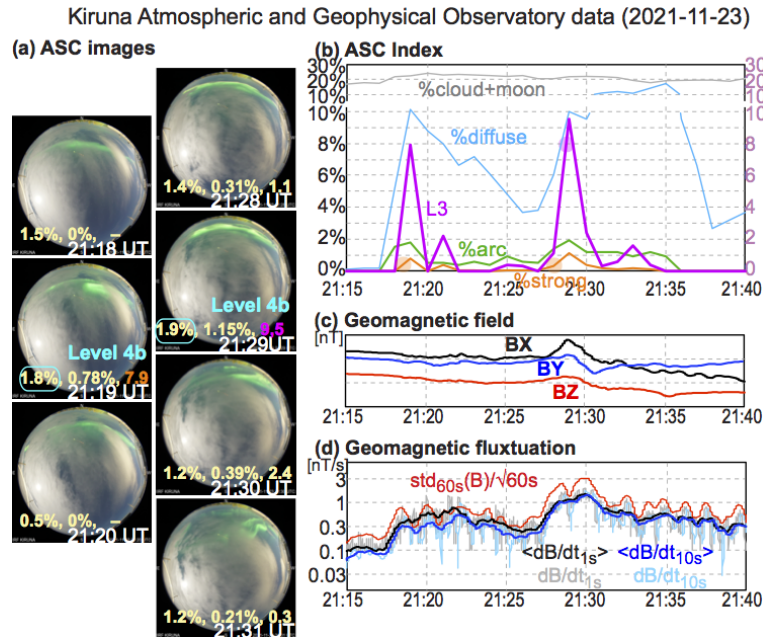


**Figure 10.** The same as Figure 5 for the Level 4b auroral activity at 21:29 UT on 23 November, 2021. The automatic exposure time is 4s at 21:19 and 3s at 21:29 UT.

320 Another advantage of the present method (expert system) is that we just have to adjust the criterion for different ASCs at different locations that have different light conditions, different morphology (due to latitudinal difference), and for different camera manufactures/models that have different colour characteristics. The goal is again too obtain the similar ASC auroral index values for the same level of activity. By doing so, the second step can be processed with the similar criterions as the present one. Below is the tasks for future improvement that we consider from the present version (ver. 1.0) in addition to  
 325 obvious task: tuning the criterion values (e.g., 2.8% instead of 3.0% for %arc in the Level 6 criterion, etc).

#### 4.1 Correction using exposure time information and UT information (ver. 1.1)

The present version is made to judge only from the jpeg image (without using hidden information) such that the analyses code (see supplemental material) can be easily modified for the other ASC jpeg images. However, if limited to Kiruna, we can use two extra information that is available. One is UT information that is tagged to the jpeg image. The other is exposure time given  
 330 as hidden information of the jpeg file (can be extracted with "exiftool" command for python program). So far we have managed to identify the brightening of aurora (Level 6) for different UT and for different exposure time, but both the ASC auroral index and activity level definition will be improved by including these information. For example, postmidnight diffuse aurora during a substorm is often strong enough to be misjudged as the auroral arc (category "green arc") although such an overestimation does not effect the judgement of Level 6 and Level 4b very much. These improvements require further subdivision of auroral



335 image in terms of UT and exposure time, which requires much more auroral examples to examine than what we have used so far.

#### 4.2 N<sub>2</sub> red (670 nm) line (ver. 1.2)

In the present version, all auroral pixel must satisfy  $R < G$  and  $B < G$  (criterion on H means this relation) to avoid any contamination from white light or twilight. This automatically removes the strong red line by N<sub>2</sub> mission (670 nm: mainly < 100 km  
340 altitudes) or faint blue line by N<sub>2</sub><sup>+</sup> emission (428 nm: mainly > 150 km altitude). Adding these lines, particularly strong N<sub>2</sub> red line, would improve the "strong aurora" definition. One possibility is to examine more examples with strong N<sub>2</sub> red lines (they are rare) to find out GRB colour code difference from the twilight, moon, and other light sources. This is not impossible because some a limited area in the R-G-B space has been defined. The other possibility is to include the UT information and location of the pixel such that we can exclude the twilight before the analyses. Priority is lower for the N<sub>2</sub><sup>+</sup> blue line than the  
345 N<sub>2</sub><sup>+</sup> red line because appears more often near the equinoxes than winter, and including the N<sub>2</sub><sup>+</sup> blue line may cause inequality between different seasons.

#### 4.3 Moon filter and twilight filter (ver. 1.3)

To reduce the moon effect, we currently mask all pixels within a radius that is 14 times the detected moon radius (even the radius of the moon changes with time, location, and moon phase) because both the sky and the all-sky dome scatters the  
350 moonlight, modifying the colour and intensity of the auroral pixels in a wide area around the moon during almost all moon phases. Of course the moon itself blocks the aurora at its vicinity.

Just masking the moon from date and time is not easy because the all-sky dome modifies the moon location and size. Also, the effect (shift of the colour toward blue) is seen at almost all pixels. One possible counterpart is to use "corrected B" values which is reduced from the obtained B value, depending on the distance from the moon. The optimum correction needs  
355 examination of more samples of aurora with the moon. We can make the similar correction for the twilight, but this is not as urgent as the moon correction because the twilight problem is seen only at the beginning and end of the season when the nighttime is very short.

#### 4.4 Defining less intense but sudden intensification as Level 5 (ver. 1.4)

Some Local-Arc-Breakings are more compact and less intense than others. Some of them are even difficult to distinguish from  
360 simple intensification or deformation of auroral arcs, e.g., expansion of bright region or really the breaking but soon back to the arc again. Therefore, it would be useful to have a category of minor sudden intensification as Level 5. Such introduction of "fuzziness" makes the alert system more reliable.



#### 4.5 Dividing field-of-view (ver. 2)

The present ASC aurora index treats all pixels equal, which makes the zenith aurora is eventually weighted more in the calculation of the index values than the other part of the sky due to the geometric effect. Furthermore, the Local-Arc-Breaking in the south sky expands toward the entire sky, giving higher values than the Local-Arc-Breaking in the northern sky that expands mainly toward northern edge. These "auroral location" problems (reliable only near the zenith or slightly south) should ideally be solved by placing many ASCs within 100 km distance each other. Meanwhile, we can make some improvement with a single ASC by dividing the field-of-view (FOV) into two-three areas (north, middle, south) and obtaining the index values for each areas. When calculating the final index values, we can weight more on the northern sky. The detailed scheme needs tuning after examining more samples.

#### 4.6 Previous 5-min activities (ver. 2)

For some Local-Arc-Breaking cases without the Level 6 alert, its criterion is satisfied if we take peak values of the ASC auroral index within 5 minutes (4 cases out of 8 nights in Table 10). On 8 Feb, 2022, L3 and %strong are well above the Level 6 criterion at 20:02 UT and 20:03 UT (but %arc = 2.6%, i.e., lower than required 3.0%), whereas %arc and %strong is satisfied at 20:06 UT but L3=6.7. On 7 March 2022, %arc was 3.9% at 18:28 UT, whereas L3 and %strong exceeded the Level 6 criterion at 18:31 UT. On 12 March 2022, L3 and %strong exceeded the Level 6 criterion at 21:45 UT, only one minute after %arc satisfied the criterion (=4.3%). Finally, on 3 April 2022 (Figure 9), the index values did not exceed Level 6 just because of %arc did not satisfy the criterion (=2.5%) at 20:06 UT and %strong did not satisfy the criterion (=0.17%) at 20:07 UT. Other values during these two images exceeded the Level 6 criterion.

These example suggest a possibility to loosen the criterion by using nearby data. Other possible solution is to introduce gradients of values such that sharp increases of %strong and L3 as the condition to ease the criterion. Such attempts are also useful in defining Level 5 and lower level of activities. Problem is that the optimization requires complicated examinations of multi-minutes data, and finding the solution is not simple.

#### 4.7 Precursor or Level 4 (ver. 2)

As the extension of the previous task (considering previous 5-min activity), we can even search precursor signatures of the Local-Arc-Breaking. Level-4a and Level-4b are defined as the first step for this effort, and the methods mentioned above will help tuning Level 4. For this part, using neural network is another option. Here, the neural network should be applied only on the ASC index values of past 10 minutes to predict Level 6 activity. The we can define the ASC auroral index values between 5 min before the Level 6 and 10 min before the Level 6 can be a good candidate of set of values corresponds to Level 4.

#### 4.8 Adding geomagnetic variation (ver. 3)

As an external index, geomagnetic activity can be used to help defining the level. To evaluate the optimum information for this purpose, we showed geomagnetic variations in Figures 4-8 and 10 in both DC and AC format. As the AC variation, we



395 showed dB/dt values obtained from 1-sec values and from 10-sec values, and their 1-min running averages, respectively. We also showed theoretical accuracy of the 1-sec values, i.e., standard deviation divided by square root of 60s, giving the result with the same unit [nT/s] as other parameters.

Change in Bx (deviation within 10 minutes or so) is the optimum parameter for DC variation, whereas all AC profiles are similar to each other, suggesting that using 10-sec values is sufficient as the source data when 1s resolution data is not available. On this other hand, the standard deviation method might be optimum if the computation time is short enough. To find out the optimum one, we need to examine more cases, which needs another solid analyses (e.g., Juusola et al., 2020). This problem is directly related to the geomagnetically induced current (GIC) during the spaceweather hazard events. That is, we can even search for possible precursor of the big GIC events (big dB/dt events) in the ASC index.

## 5 Summary and conclusion

We developed an automatic identification scheme of sudden and significant intensification of auroral arc with expanding motion (Local-Arc-Breaking) seen in the ASC jpeg image, and applied it for real-time alert. Unlike the other automatic identification such as using the neural network, we used a set of simple criterions and calculations (expert system). The scheme is divided into two steps: (1) obtaining a set of simple numbers that represents the sky condition of the entire ASC (150000 active pixels with 256×256×256 colour values each), which we call the ASC auroral index, and (2) judging the auroral activity level only from the index values. The midterm product (ASC auroral index) is stored on realtime bases, whereas the result of activity assessment is sent only as warning email real-time when the index values satisfy a criterion "Level 6". The alert system started 5 November, 2021.

The first step is further divided into two stages: (1a) pixel-to-pixel classification into "strong aurora", most likely auroral arc (category "green arc"), most likely visible diffuse aurora (category "visible diffuse"), most likely "cloud", most likely "the moon", most likely "artificial light" using just R, G, B, and H values (where H is calculated from RGB values), and (1b) simple calculation such as the percentage of the occupying area (pixel coverage) and the characteristic intensity of "strong aurora" (take average of the most luminous 4700 pixels).

The present scheme is only just version 1, and there are many room for improvement. Nevertheless, after 5 months of the operation until the end of the season, this algorithm made alert of the Local-Arc-Breaking within 10 min from when the actual brightening of aurora is detected for nearly 90% of cases (cf. Table 10). Like the false positive, false negative was also very little.

Nevertheless, there are many rooms to improve the algorithm, thanks to the present method with the explicit criterions and calculations. We listed these tasks toward future improvement.



**Table A1.** Version 0.0 criterion of ASC auroral index for old ASC (Nikon D700)

classification	condition 1	condition 2	condition 3
strong aurora:	$0.20 < H < 0.46$	$0.20 < S < 0.8$	$0.20 < L < 0.8$
green arc:	$0.18 < H < 0.46$	$0.15 < S < 0.8$	$0.10 \leq L < 0.8$
visible diffuse:	$0.16 < H < 0.50$	$0.10 < S < 0.8$	$0.5 \leq L < 0.8$
cloud:	$H < 0.16$	$0.10 < S < 0.8$	$0.15 < L < 0.8$

**Table A2.** Version 0.1 criterion of ASC auroral index for old ASC (Nikon D700)

classification	condition 1	condition 2	condition 3
strong aurora:	$0.20 \leq H < 0.46$	$0.17 \leq S < 0.8$	$0.30 \leq L < 0.83$
green arc:	$0.18 \leq H < 0.46$	$0.13 \leq S < 0.8$	$0.15 \leq L < 0.83$
visible diffuse:	$0.16 \leq H < 0.57$	$0.09 \leq S < 0.8$	$0.5 \leq L < 0.83$
cloud:	$H < 0.16$	$0.10 \leq S < 0.8$	$0.15 \leq L < 0.83$

### Appendix A: Version 0 classification using only HSL values

For the old KAGO's ASC (Nikon D700 camera) until April 2020, we used less accurate classification method using only HSL  
 425 values only to obtain the ASC auroral index version 0 (Yamauchi et al., 2018). In this version, we just plotted the index values  
 in our website in the real-time bases, and its archive is found at: [https://www2.irf.se/maggraphs/aurora\\_detect/graphs/](https://www2.irf.se/maggraphs/aurora_detect/graphs/). For this  
 real time operation, we used criterion (version 0.0) that is summarised in Table A1.

This version (version 0.0) was slightly updated for the data analyses when the operation of the old ASC (Nikon D700  
 camera) is finished. The revised criterion (version 0.1) is summarised in Table A2.

430 *Code availability.* Python code is found in the supplemental material (except sending email alert part which includes private informations)

*Data availability.* The all sky images and magnetic field data are publicly available at IRF's observatory data site <https://www.irf.se/en/about-irf/data/>, with ASC data at <https://www.irf.se/alis/allsky/krn/>, magnetic field data at <https://www.irf.se/maggraphs/iaga/>, and ASC auroral index at <https://www.irf.se/alis/allsky/nowcast/>.

*Author contributions.* MY is responsible all part except the calibration, maintenance and optimum setting of the ASC, for all of which UB  
 435 is responsible



<https://doi.org/10.5194/egusphere-2022-331>

Preprint. Discussion started: 17 May 2022

© Author(s) 2022. CC BY 4.0 License.



*Competing interests.* no competing interest

*Acknowledgements.* Maintenance of system including software is done by members of Kiruna Atmospheric and Geophysical Observatory (KAGO) at IRF. We also thank Dennis van Dijk for developing preliminary version (version 0) made for the old Nikon D700 camera.



## References

- 440 Akasofu, S.-I.: The development of the auroral substorm, *Planet. Space Sci.*, 12, 273-282, DOI = 10.1016/0032-0633(64)90151-5, 1964.
- Friis-Christensen, E., McHenry, M. A., Clauer, C. R., and Vennerstrom, S.: Ionospheric traveling convection vortices observed near the polar cleft: a triggered response to sudden changes in the solar wind, *Geophys. Res. Lett.*, 15, 253-256, DOI = 10.1029/GL015i003p00253, 1988.
- Juusola, L., Vanhamäki, H., Viljanen, A., and Smirnov, M.: Induced currents due to 3D ground conductivity play a major role in the interpretation of geomagnetic variations, *Ann. Geophys.*, 38, 983-998, DOI = <https://doi.org/10.5194/angeo-38-983-2020>, 2020.
- 445 Kvammen, A., Wickstrøm, K., McKay, D., and Partamies, N.: Auroral image classification with deep neural networks. *J. Geophys. Res.*, 125, e2020JA027808, DOI=10.1029/2020JA027808, 2020.
- Luhr, H., Aylward, A., Bucher, S.C., Pajunpaa, A., Pajunpaa, K., Holmboe, T., and Zalewski, S.M.: Westward moving dynamic substorm features observed with the IMAGE magnetometer network and other ground-based instruments, *Ann. Geophys.*, 16, 425-440, DOI=10.1007/s00585-998-0425-y, 1998.
- 450 Nanjo, S., Satonori Nozawa, S., Yamamoto, M., Kawabata T., Johnsen, M.G., Tsuda, T.T, Hosokawa, K.: An a auroral detection system using deep learning: real-time operation in Tromsø, Norway, DOI=10.21203/rs.3.rs-1090985/v1, 2021.
- Partamies, N., O. Amm, K. Kauristie, T. I. Pulkkinen, and E. Tanskanen, A pseudo-breakup observation: Localized currentwedge across the postmidnight auroral oval, *J. Geophys. Res.*, 108(A1), 1020, DOI=10.1029/2002JA009276, 2003.
- 455 Sigernes, F., Holmen, S. E., Biles, D., Bjørklund, H., Chen, X., Dyrland, M., Lorentzen, D. A., Baddeley, L., Trondsen, T., Brändström, U., Trondsen, E., Lybekk, B., Moen, J., Chernouss, S., and Deehr, C. S.: Auroral all-sky camera calibration, *Geosci. Instrum. Method. Data Syst.*, 3, 241-245, DOI=10.5194/gi-3-241-2014, 2014.
- Syrjäso, M.T., Pulkkinen, T.I., Janhunen, P., Viljanen, A., Pellinen, R.J., Kauristie, K., Opgenoorth, H.J., Wallman, S., Eglitis, P., Karlsson, P., Amm, O., Nielsen, E., and Thomas, C.: Observations of substorm electrodynamics using the MIRACLE network, in *Substorms-4*, edited by Kokubun S., and Kamide, Y., Terra Scientific Publishing Company, Tokyo, 111-114, 1998
- 460 Yamauchi, M., Brandstrom, U., van Dijk, D., Sergienko, T., and Kero, J.: Improving nowcast capability through automatic processing of combined ground-based measurements, in *EGU General Assembly Conference Abstracts*, p. 1779, 2018.